AMERICAN SOCIETY FOR MICROBIOLOGY | Infection and Immunity®

CELLULAR MICROBIOLOGY:
PATHOGEN-HOST CELL MOLECULAR INTERACTIONS

Activation of ASC Inflammasome Driven by Toll-Like Receptor 4 Contributes to Host Immunity against Rickettsial Infection

Claire Rumfield,[a] Ilirjana Hyseni,[a] Jere W. McBride,[a,b,c] David H. Walker,[a,b,c] Rong Fang[a,b,c]

[a]Department of Pathology, University of Texas Medical Branch, Galveston, Texas, USA
[b]Center for Biodefense and Emerging Infectious Diseases, University of Texas Medical Branch, Galveston, Texas, USA
[c]Institute for Human Infections and Immunity, University of Texas Medical Branch, Galveston, Texas, USA

ABSTRACT Rickettsiae are cytosolically replicating, obligately intracellular bacteria causing human infections worldwide with potentially fatal outcomes. We previously showed that *Rickettsia australis* activates ASC inflammasome in macrophages. In the present study, host susceptibility of ASC inflammasome-deficient mice to *R. australis* was significantly greater than that of C57BL/6 (B6) controls and was accompanied by increased rickettsial loads in various organs. Impaired host control of *R. australis in vivo* in ASC$^{-/-}$ mice was associated with dramatically reduced levels of interleukin 1β (IL-1β), IL-18, and gamma interferon (IFN-γ) in sera. The intracellular concentrations of *R. australis* in bone marrow-derived macrophages (BMMs) of TLR4$^{-/-}$ and ASC$^{-/-}$ mice were significantly greater than those in BMMs of B6 controls, highlighting the important role of inflammasome and these molecules in controlling rickettsiae in macrophages. Compared to B6 BMMs, TLR4$^{-/-}$ BMMs failed to secrete a significant level of IL-1β and had reduced expression levels of pro-IL-1β in response to infection with *R. australis*, suggesting that rickettsiae activate ASC inflammasome via a Toll-like receptor 4 (TLR4)-dependent mechanism. Further mechanistic studies suggest that the lipopolysaccharide (LPS) purified from *R. australis* together with ATP stimulation led to cleavage of pro-caspase-1 and pro-IL-1β, resulting in TLR4-dependent secretion of IL-1β. Taken together, these observations indicate that activation of ASC inflammasome, most likely driven by interaction of TLR4 with rickettsial LPS, contributes to host protective immunity against *R. australis*. These findings provide key insights into defining the interactions of rickettsiae with the host innate immune system.

KEYWORDS inflammasome, rickettsiae, TLR4, ASC, LPS

Rickettsiae are obligately intracytosolic Gram-negative bacteria that reside in an arthropod host during a part of their zoonotic cycle. Spotted fever group (SFG) rickettsiae, such as *Rickettsia rickettsii* and *Rickettsia conorii*, are transmitted through the bite of an infected tick and can cause a group of human diseases with a continuous spectrum of severity of illness and overlapping clinical manifestations, some of which are potentially life-threatening. Tick-borne diseases increasingly threaten the health of residents in the United States due to their significantly increased incidence and potential for a fatal or severe outcome. SFG rickettsiae were responsible for 16,807 cases of probable or confirmed infections in the United States during 2010 to 2015 (1). Fatal cases of Rocky Mountain spotted fever, caused by *R. rickettsii*, were reported along the United States-Mexico border from 2013 to 2016 (2). Development of an effective vaccine against rickettsial diseases has not been achieved, at least partially due to the incomplete understanding of how rickettsiae are recognized by infected innate immune cells.

In general, a pathogen is initially recognized by pattern recognition receptors (PRRs),

Citation Rumfield C, Hyseni I, McBride JW, Walker DH, Fang R. 2020. Activation of ASC inflammasome driven by Toll-like receptor 4 contributes to host immunity against rickettsial infection. Infect Immun 88:e00886-19. https://doi.org/10.1128/IAI.00886-19.

Editor Guy H. Palmer, Washington State University

Address correspondence to Rong Fang, rofang@utmb.edu.

Received 26 November 2019
Returned for modification 9 December 2019
Accepted 23 January 2020

Accepted manuscript posted online 3 February 2020
Published 23 March 2020

such as Toll-like receptors (TLRs) and nucleotide-binding oligomerization domain (NOD)-like receptors (NLRs) (3). PRRs are expressed by most innate immune effector cells, such as macrophages. PRRs recognize and bind to pathogen-associated molecular patterns (PAMPs) or damage-associated molecular patterns (DAMPs) to trigger the innate immune responses to the pathogen. Among different TLRs, TLR4 is known to recognize lipopolysaccharides (LPS) in association with MD2 and CD14. This recognition scenario has been hypothesized to occur in rickettsiae as well (4). However, the direct interaction of rickettsial LPS with TLR4 and its downstream signaling have never been studied. Inflammasomes are cytosolic multiprotein complexes assembled by NLRs and apoptosis-associated speck-like protein containing a CARD (PYCARD, also known as ASC). ASC acts as a molecular bridge between activated inflammasome sensors and the effector protein pro-caspase-1. We recently demonstrated that *Rickettsia australis* activates inflammasome in macrophages, as evidenced by cleavage of caspase-1 and secretion of caspase-1-dependent interleukin 1β (IL-1β) and IL-18 (5). ASC is an essential component in inflammasome activation by *R. australis* in mouse macrophages. NLRP3 only partially accounts for the cytosolic recognition of *R. australis* by inflammasome in mouse macrophages and is dispensable for host control of infection *in vivo* (5). Thus, the role of inflammasome in mediating the interactions of rickettsiae with mammalian hosts *in vivo* remains elusive.

Activation of NLRP3 inflammasome in macrophages requires two steps: priming and activation (6–8). The priming step (signal 1) is provided by inflammatory stimuli such as TLR4 agonists, which induce NF-κB-mediated NLRP3 and pro-IL-1β expression, and the activation step (signal 2) is triggered by PAMPs and DAMPs, thereby promoting NLRP3 inflammasome assembly and caspase-1-mediated IL-1β and IL-18 secretion (7, 8). Furthermore, intracellular LPS derived from Gram-negative bacteria can be directly recognized by caspase-11, -4, and -5, independent of TLR4 (6, 9, 10). LPS is a component of the outer membrane in the cell envelope of rickettsiae, which are cytosolically replicating, Gram-negative bacteria. We aim to pursue identifying the essential signals driving rickettsial activation of inflammasome. Does LPS of *R. australis* interact with macrophages via a TLR4-dependent or TLR4–independent mechanism? Answering this question will increase our understanding of the molecular mechanisms involved in canonical versus noncanonical inflammasome activation by rickettsiae.

Although microvascular endothelial cells are the main targets of disseminated infection, macrophages are most likely the initial target cells for rickettsiae in the tick feeding site (11–13). Previous studies have demonstrated that innate immune signaling and macrophages play a critical role in controlling rickettsial infection (5, 11, 14–17). *R. australis* is the etiologic agent of potentially fatal Queensland tick typhus and a member of tick-borne rickettsiae carrying SFG LPS. B6 background mice enable us to study the mechanisms of host immunity to SFG rickettsiae *in vivo* using genetically modified mice. *Rickettsia australis*-infected B6 mice were recently employed to investigate the mechanisms of host protective immunity and the interactions of rickettsiae with macrophages (5, 18–20). Previous studies using other animal models of rickettsial infection have identified the critical roles of gamma interferon (IFN-γ), cytotoxic CD8 T cells, MyD88, and TLR4 in protective immunity against rickettsiae (16, 17, 21–23).

In the present study, we sought to investigate the mechanisms by which rickettsiae activate inflammasome by employing *R. australis*-infected macrophages from TLR4$^{-/-}$ and ASC$^{-/-}$ mice as well as in an experimental *in vivo* model of rickettsioses. Our studies revealed that rickettsial LPS acts as a priming signal for ASC-dependent inflammasome activation through TLR4 in macrophages, which contributes to bacterial clearance by IL-1β-mediated rickettsial killing. Our data indicated that ASC inflammasome plays a pivotal role in recognition and control of infection by *R. australis* in an experimental model of the disease.

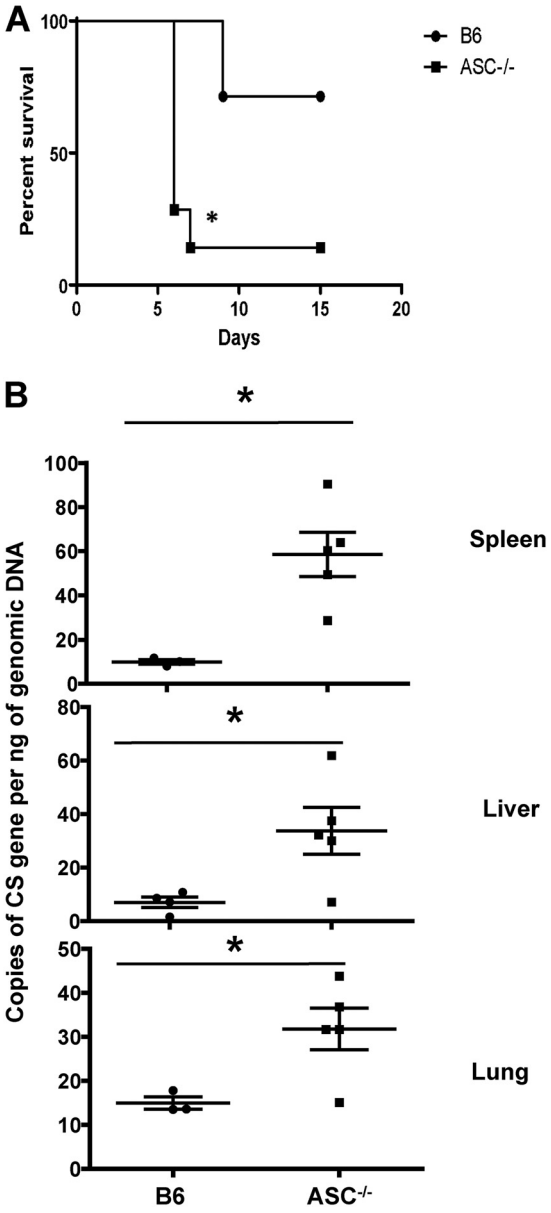

FIG 1 ASC inflammasome contributes significantly to host susceptibility to and *in vivo* clearance of *R. australis*. (A) B6 and ASC$^{-/-}$ mice were inoculated with 0.5 LD_{50} of *R. australis* i.v. Host survival was monitored daily until day 20 p.i. Each group of mice included 6 to 10 mice. (B) On day 4 p.i., mice were sacrificed, and the concentrations of rickettsiae in spleens, livers, and lungs were quantified by real-time PCR. Data are means ± standard errors (SE) for 5 mice for each group. Data represent two independent experiments. *, $P < 0.05$ for a significant difference between B6 and ASC$^{-/-}$ mice.

RESULTS

ASC inflammasome mediates host resistance to *R. australis* by facilitating *in vivo* clearance of bacteria. The *in vivo* contribution of inflammasome to host protective immunity is not completely understood. To address this question, we challenged ASC$^{-/-}$ mice with *R. australis* at 0.5 50% lethal dose (LD_{50}) for B6 mice. As shown in Fig. 1A, 90% of ASC$^{-/-}$ mice succumbed to infection on day 7 postinfection (p.i.) while only 25% of B6 mice died on day 9 p.i. These results suggest that ASC inflammasome contributes to host resistance against *R. australis*. To investigate the mechanisms involved in ASC inflammasome-mediated host protection against rickettsiae, we determined the bacterial loads in tissues of these infected mice. On day 4 p.i., the concentrations of *R. australis*, determined by the number of copies of *gltA* per nanogram of

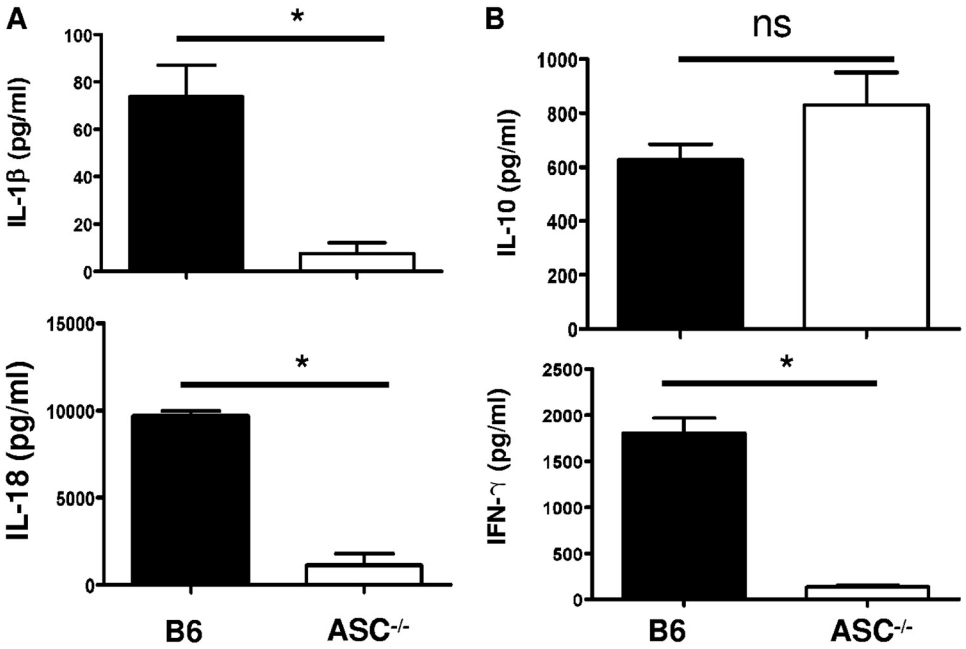

FIG 2 ASC inflammasome is indispensable for significant serum levels of inflammasome-mediated cytokines during rickettsial infection. B6 and ASC$^{-/-}$ mice were inoculated with 0.5 LD_{50} of *R. australis* i.v. On day 4 p.i., mice were sacrificed. (A) The *in vivo* production of inflammasome-mediated cytokines, including IL-1β and IL-18, was assessed in sera by ELISA. (B) Serum levels of IL-10 and IFN-γ were measured by ELISA. Results are means $\pm$ SE of data from 4 to 8 mice per group. Data represent two independent experiments. ns, not significant. *, $P < 0.05$ for a significant difference between B6 and ASC$^{-/-}$ mice.

genomic DNA, in infected spleens, livers, and lungs of infected ASC$^{-/-}$ mice were all significantly greater than the counterparts in B6 mice (Fig. 1B). These results revealed that ASC greatly contributed to host control of *R. australis* infection *in vivo*.

Next, we measured the *in vivo* production of cytokines, including inflammasome-dependent IL-1β and IL-18 and inflammasome-independent IFN-γ and IL-10, on day 4 p.i. in the sera of *R. australis*-infected B6 and ASC$^{-/-}$ mice. Indeed, the levels of IL-1β and IL-18 in the sera of infected ASC$^{-/-}$ mice were significantly lower than those in B6 mice (Fig. 2A). No significant difference in the serum levels of IL-10, used as a control, was observed in infected B6 and ASC$^{-/-}$ mice (Fig. 2B). Interestingly, we found a significantly lower level of IFN-γ in the sera of *R. australis*-infected ASC$^{-/-}$ mice than in those of B6 mice (Fig. 2B). These results suggest that the *in vivo* production of IL-1β and IL-18 is ASC dependent during rickettsial infection. It is most likely that the *in vivo* production of IFN-γ in murine spotted fever rickettsioses is associated with ASC-mediated immune events. Thus, our results suggest that ASC inflammasome mediates host protective immune responses against *R. australis* by facilitating the bacterial clearance in varied organs, which is associated with a greater level of inflammasome-dependent cytokines in serum. Evaluation of histopathological changes in livers of infected B6 and ASC$^{-/-}$ mice compared to uninfected controls (Fig. 3I) showed hepatic lobular and perivascular foci of macrophages and polymorphonuclear neutrophils (PMNs) with hepatocellular dropout (Fig. 3IIA to E). Numerous associated apoptotic hepatocytes were observed in the livers of infected B6 and ASC$^{-/-}$ mice. Hepatic coagulative necrotic infarcts were detected in infected ASC$^{-/-}$ mice but not in infected B6 mice (Fig. 3IIF and G). Although infected spleens from these two strains of mice both showed prominent periarteriolar lymphocytic sheaths, infected spleens of B6 mice had clusters of macrophages and PMNs in red pulp, while infected spleens of ASC$^{-/-}$ mice had clusters of only macrophages in red pulp (Fig. 3IIIH to K). These results suggest that ASC is involved in regulating the inflammatory responses in tissues induced by infection with *R. australis in vivo*.

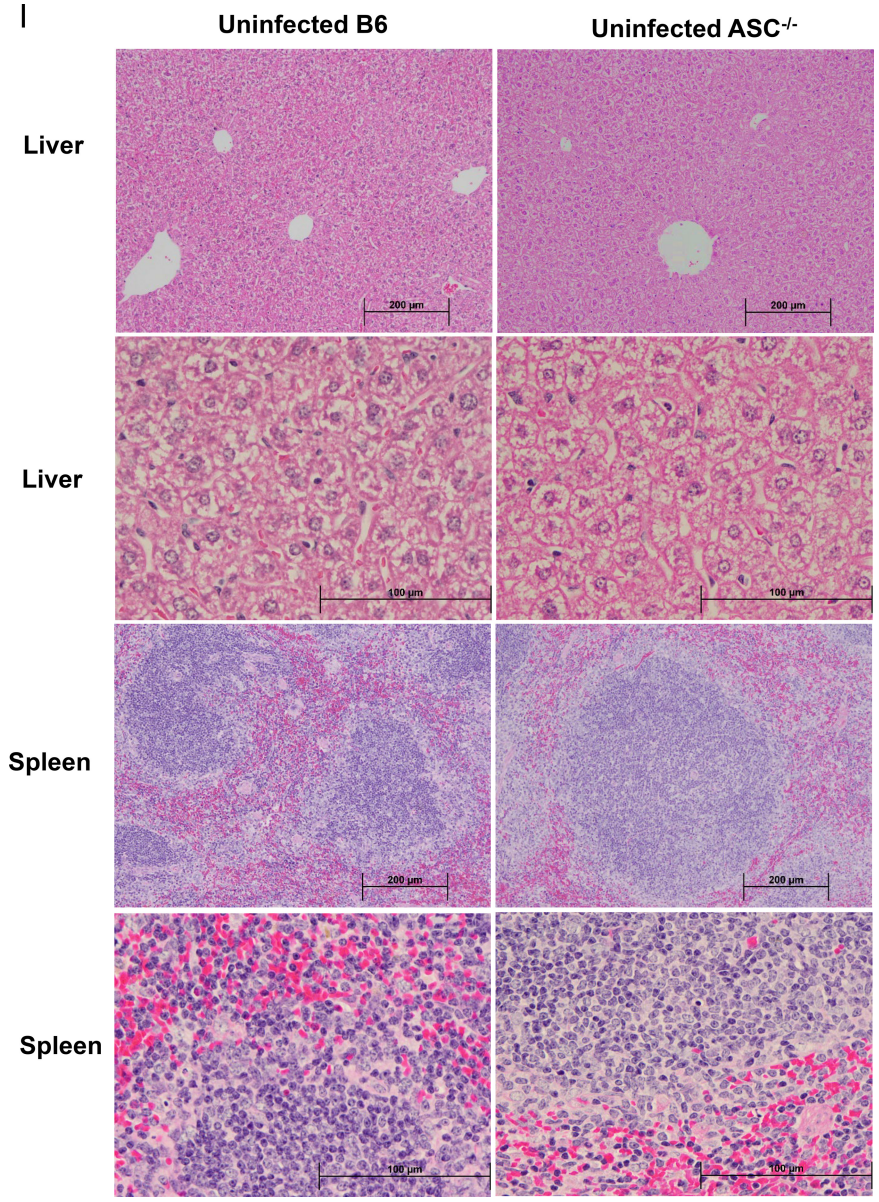

FIG 3 Histopathological analysis of tissues of *R. australis*-infected B6 and ASC$^{-/-}$ mice. B6 and ASC$^{-/-}$ mice were inoculated with 0.5 LD_{50} of *R. australis* i.v. On day 4 p.i., mice were euthanized, and tissues were collected. (I) As negative controls, uninfected B6 and ASC$^{-/-}$ mice were monitored and euthanized along with the infected mouse groups. Histopathological analysis of livers and spleens was performed at magnifications of ×10 (scale bar, 200 μm) and ×40 (scale bar, 100 μm). (II) (A and B) Foci of inflammatory cells in liver tissue (arrows). (C to E) Perivascular infiltration (arrows) and polymorphonuclear neutrophils (PMNs) (arrowheads) in livers. (F and G) Coagulative necrotic infarct (arrowheads) only in livers of infected ASC$^{-/-}$ mice and surrounding inflammation and tissue repair (arrows). (III) (H to K) Spleens of infected B6 and ASC$^{-/-}$ mice. Clusters of macrophages and normal periarteriolar lymphocyte sheaths, a portion of white pulp, in spleens of both groups of mice are shown. In red pulp, PMNs (arrowheads) were found only in infected B6 mice (H and J), not in infected ASC$^{-/-}$ mice (I and K).

Contributions of inflammasome elements to elimination of intracellular *R. australis* in macrophages. To determine the mechanisms by which ASC inflammasome mediates the clearance of *R. australis* in infected tissues, we determined the contribution of ASC and TLR4 to host clearance of *R. australis* in BMMs *in vitro*. As shown in Fig. 4A, compared to B6 BMMs, BMMs from ASC$^{-/-}$ mice had significantly greater concentrations of intracellular *R. australis*, suggesting that ASC contributes to the clearance of intracellular rickettsiae in macrophages. Although TLR4 has been reported

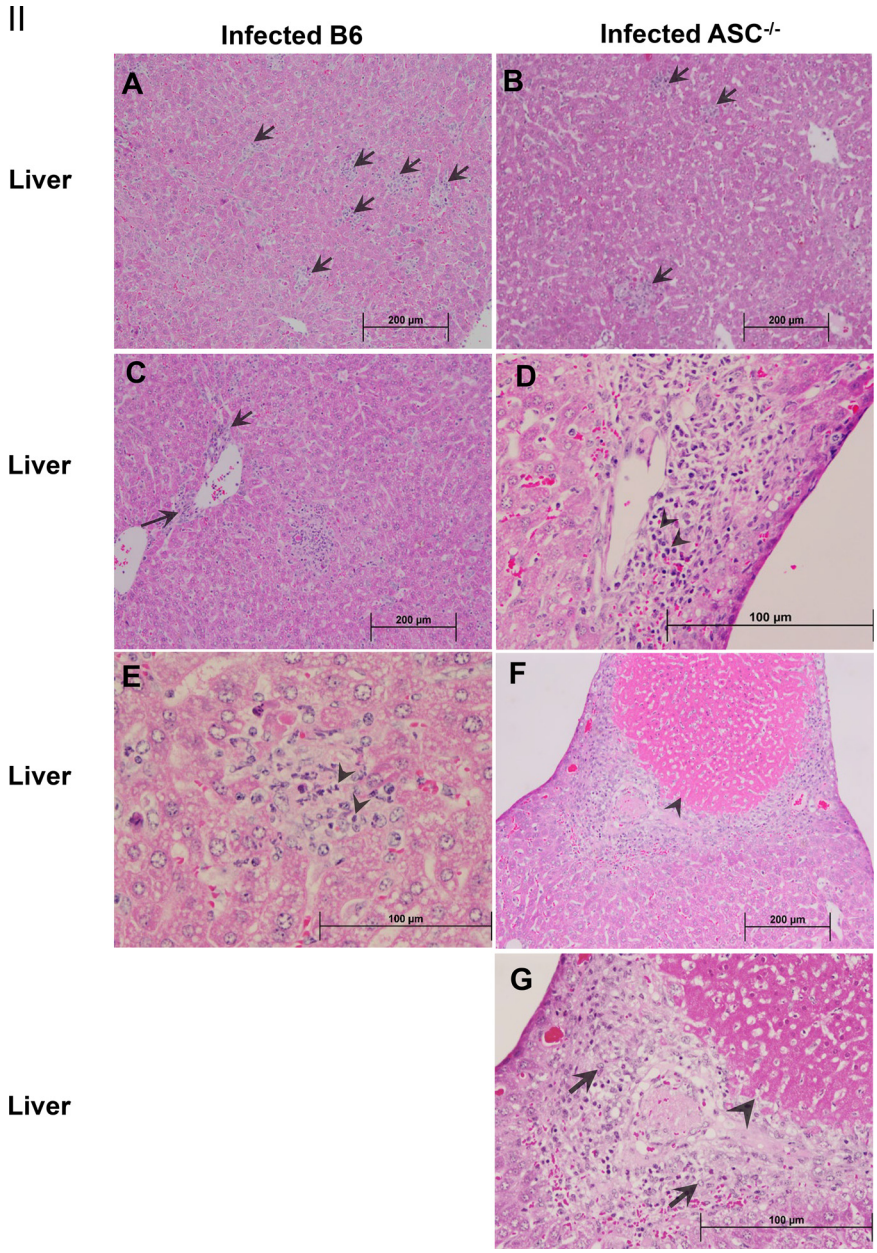

FIG 3 (Continued)

to mediate host protective immunity against *R. conorii* in the mouse model of rickettsioses (14–16), the cellular mechanisms involved are not completely understood. To investigate whether TLR4 contributes to host control of *R. australis* in macrophages, we determined the bacterial concentrations in BMMs of TLR4$^{-/-}$ mice. Interestingly, the intracellular concentrations of *R. australis* in BMMs of TLR4$^{-/-}$ mice were significantly greater than those in B6 BMMs (Fig. 4B). These results highlighted the idea that the elements potentially involved in activation of inflammasome, ASC and TLR4, contribute significantly to host clearance of *R. australis* in BMMs, which is consistent with our *in vivo* data (Fig. 1).

Next, we treated RAW 264.7 macrophages with recombinant IL-1β to determine whether IL-1β exhibits a rickettsicidal effect. As shown in Fig. 4C, the concentrations of intracellular *R. australis* in RAW 264.7 macrophages treated with recombinant IL-1β were significantly reduced compared to those in untreated controls. These results

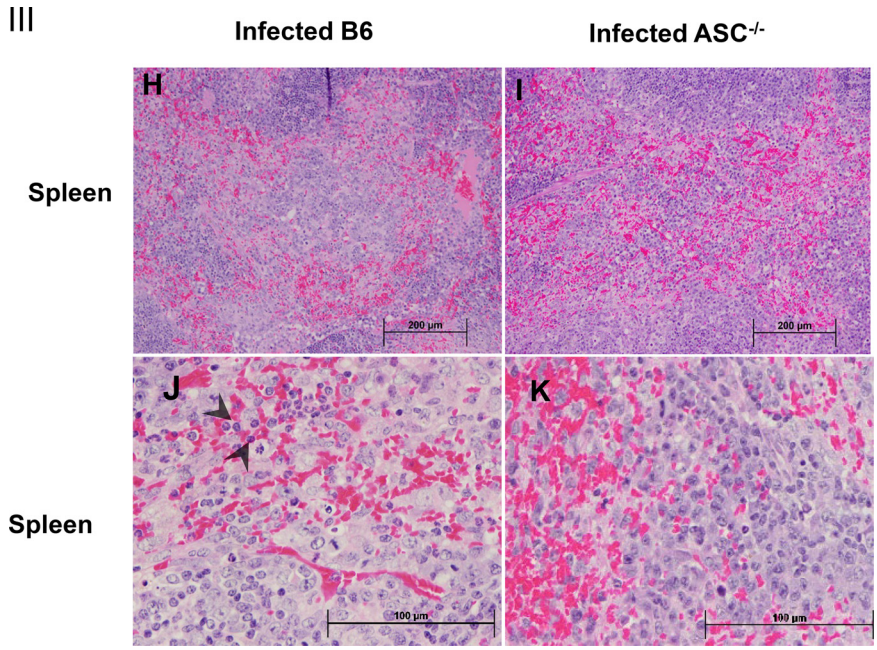

FIG 3 (Continued)

demonstrated that IL-1β played a part in driving the rickettsicidal activity, at least in macrophages, which is consistent with our previous results on primary mouse macrophages (11). Thus, our results clearly elucidated that inflammasome elements, including the adaptor (ASC), the product (IL-1β), and possibly the priming signal (TLR4), contributed greatly to the host control of intracellular *R. australis* in mouse macrophages.

Mechanisms of ASC inflammasome activation by *R. australis* in macrophages. To investigate how the upstream signals mediate the synthesis of pro-IL-1β in *R. australis*-infected macrophages, we determined the secretion levels of IL-1β and expression of pro-IL-1β in *R. australis*-infected BMMs of B6 mice and of selected knockout mice. Isolated BMMs stimulated with *Salmonella* LPS and ATP served as a positive control. As shown in Fig. 5A, *R. australis*-infected TLR4$^{-/-}$ BMMs failed to produce a significant amount of IL-1β upon infection, suggesting that ASC inflammasome-mediated secretion of IL-1β by *R. australis*-infected BMMs is TLR4 dependent. To further investigate how TLR4 signals the activation of inflammasome, we measured the secretion of IL-1β in MyD88$^{-/-}$ BMMs. As shown in Fig. 5B, we observed that IL-1β, although present, was present at significantly lower concentrations in MyD88$^{-/-}$ BMMs than B6 BMMs. These results suggest that IL-1β secretion, resulting from inflammasome activation by *R. australis*, is driven by the TLR4 signal via both MyD88-dependent and MyD88-independent mechanisms.

Next, we investigated the priming signal involved in activation of inflammasome by rickettsiae. Compared to untreated controls, *Salmonella* LPS and ATP, agonists for NLRP3 inflammasome, significantly increased the expression levels of pro-IL-1β in B6 BMMs but not in TLR4$^{-/-}$ BMMs (Fig. 5C). Moreover, *Salmonella* LPS and ATP significantly stimulated increased expression of pro-IL-1β in ASC$^{-/-}$ BMMs compared to untreated controls, suggesting that the synthesis of pro-IL-1β by these positive-control stimulators is ASC independent. *Rickettsia australis* infection increased the expression levels of pro-IL-1β in BMMs of B6 mice compared to untreated controls (Fig. 5C). Interestingly, *R. australis*-infected ASC$^{-/-}$ BMMs also showed a significantly increased expression level of pro-IL-1β (Fig. 5C). We have demonstrated that ASC$^{-/-}$ BMMs have complete ablation of both IL-18 and IL-1β production *in vitro* when infected with *R. australis* (5). Our present results indicated that a lack of active IL-1β secretion in *R. australis*-infected ASC$^{-/-}$ BMMs is not due to the reduced or abrogated levels of

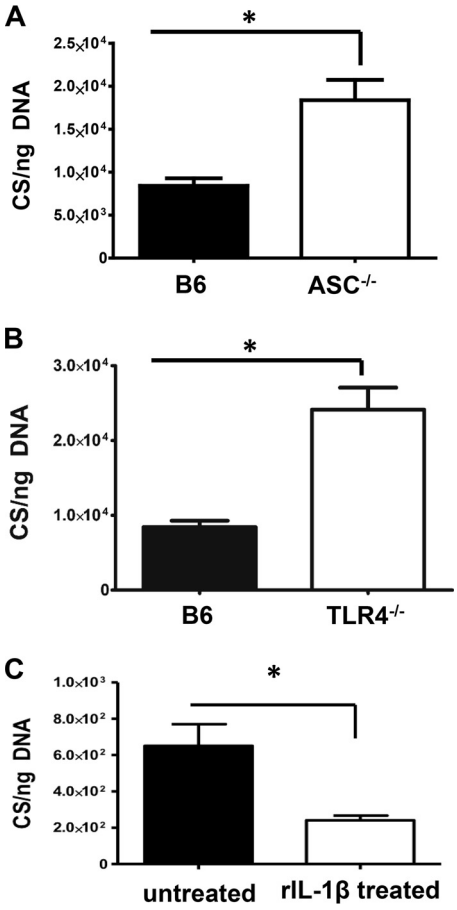

FIG 4 Contributions of inflammasome components to host control of intracellular *R. australis* in macrophages. BMMs of B6, ASC$^{-/-}$ (A), and TLR4$^{-/-}$ (B) mice were infected with *R. australis* at an MOI of 2. Fresh medium was replaced every 24 h after infection. (C) RAW 264.7 macrophages were cultured and treated with 10 ng/ml recombinant IL-1β at the time of infection. At 48 h p.i., cells were washed, and the total DNA was extracted. The concentrations of rickettsiae in these mouse macrophages were evaluated by quantitative real-time PCR at 48 h p.i. The number of citrate synthase (CS) gene copies per ng of genomic DNA represents the quantity of rickettsiae. Data represent two independent experiments. *, $P < 0.05$.

pro-IL-1β but is most likely due to the lack of cleavage of pro-IL-1β to active IL-1β. In other words, ASC was indispensable for assembly of the inflammasome complex (signal 2) during rickettsial infection. Furthermore, a significantly reduced expression level of pro-IL-1β was detected in the lysates of BMMs of TLR4$^{-/-}$ mice compared to B6 controls in response to rickettsial infection (Fig. 5C). These results indicated that *R. australis* drove the biosynthesis of pro-IL-1β via both TLR4-dependent and TLR4-independent mechanisms. Our results also suggest that ASC is involved not in priming (signal 1) but rather in assembly (signal 2) of inflammasome during *R. australis* infection.

Component of *R. australis* initiating the activation of ASC inflammasome in macrophages. We next sought to investigate which molecular component of *R. australis* is responsible for activating ASC inflammasome. We hypothesized that rickettsial LPS can activate TLR4 to serve as the first signal for ASC inflammasome activation. Compared to untreated controls, purified *R. australis* LPS with ATP stimulated a significantly increased expression level of pro-IL-1β in B6 BMMs (Fig. 5C). Compared to *Salmonella* LPS and ATP, *R. australis* LPS and ATP stimulated a reduced level of pro-IL-1β expression, suggesting that *R. australis* LPS has less potency to stimulate the biosynthesis of pro-IL-1β than *Salmonella* LPS. In addition, *R. australis* LPS and ATP led to a significant level of pro-IL-1β expression in ASC-deficient BMMs, indicating that ASC was not involved in providing priming a signal of inflammasome

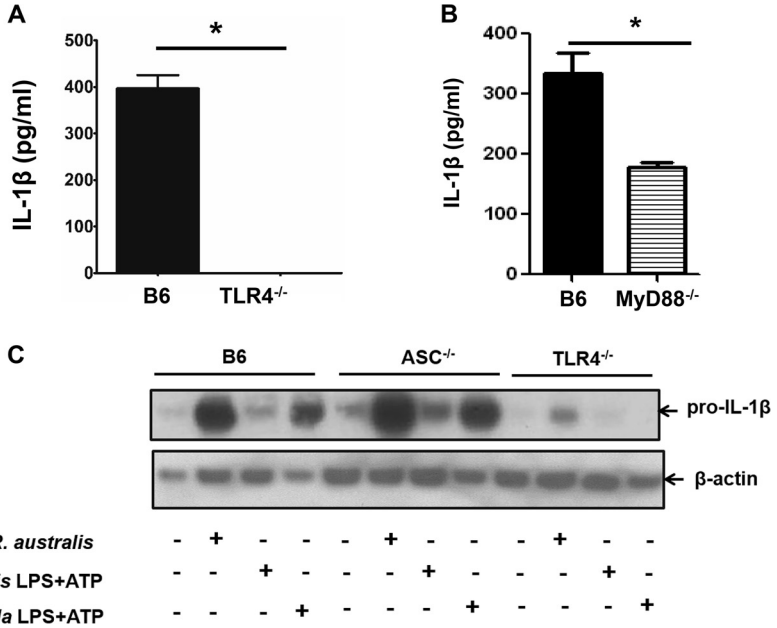

FIG 5 Mechanisms involved in mediating the secretion of IL-1β by *R. australis*-infected macrophages. BMMs were isolated from B6, TLR4$^{-/-}$, MyD88$^{-/-}$, and ASC$^{-/-}$ mice. BMMs were infected with *R. australis* at an MOI of 6 or stimulated with 50 ng/ml of purified *R. australis* LPS plus ATP for 24 h. ATP was added 1 h prior to collection. Supernatant was collected from infected BMMs of B6, TLR4$^{-/-}$ (A), and MyD88$^{-/-}$ (B) mice. Levels of secretion of IL-1β by these infected macrophages were evaluated by ELISA. (C) The synthesis of pro-IL-1β in BMMs of B6, ASC$^{-/-}$ and TLR4$^{-/-}$ mice was evaluated by specific antibodies against pro-IL-1β by immunoblotting after the cell lysates were collected. *Salmonella* LPS plus ATP served as the positive control. Data represent two independent experiments.

activation by rickettsiae. Interestingly, we did not find any expression of pro-IL-1β in TLR4$^{-/-}$ BMMs upon stimulation with *R. australis* LPS plus ATP, suggesting that rickettsial LPS activates TLR4 to promote biosynthesis of pro-IL-1β, which is the first signal for inflammasome activation (Fig. 5C).

In order to further investigate whether rickettsial LPS and ATP can activate inflammasome, we determined the activation of pro-capsase-1, active caspase-1, and active IL-1β in B6 BMMs by immunoblotting. *Salmonella* LPS-ATP served as a positive control. Cells without any treatment and cells stimulated with an inflammasome-independent cytokine, IFN-γ, served as negative controls. As described previously (24), *Salmonella* LPS and ATP stimulated significantly increased expression levels of pro-caspase-1, active caspase-1, and active IL-1β (Fig. 6A). Although IFN-γ stimulation promoted the expression of pro-caspase-1, no expression of active caspase-1 or IL-1β was detected (Fig. 6A). Compared to untreated cells, *R. australis* LPS and ATP stimulated significantly increased expression of pro-caspase-1 and slightly increased expression levels of active caspase-1 and active IL-1β. The levels of active caspase-1 and active IL-1β were significantly lower than those in cells stimulated with *Salmonella* LPS and ATP. These results suggest that *R. australis* LPS has less potency to stimulate inflammasome activation than *Salmonella* LPS. Moreover, we determined the production level of IL-1β in the supernatants of B6 and TLR4$^{-/-}$ BMMs stimulated with *R. australis* LPS and ATP by enzyme-linked immunosorbent assay (ELISA). As shown in Fig. 6B, TLR4$^{-/-}$ BMMs produced a minimum level of IL-1β upon stimulation with *R. australis* LPS and ATP which was significantly lower than that produced by B6 BMMs, suggesting that rickettsial LPS signals through TLR4 to provide the priming signal for inflammasome activation, resulting in secretion of IL-1β.

Considering the low potency of *R. australis* LPS in TLR4–ASC–caspase-1 inflammasome activation, we next primed B6 BMMs with 100 ng/ml of rickettsial LPS, in the same quantity as *Salmonella* LPS. Cells were then infected with *R. australis* followed by stimulation with ATP at the last hour prior to collection. As shown in Fig. 6C, *R. australis*

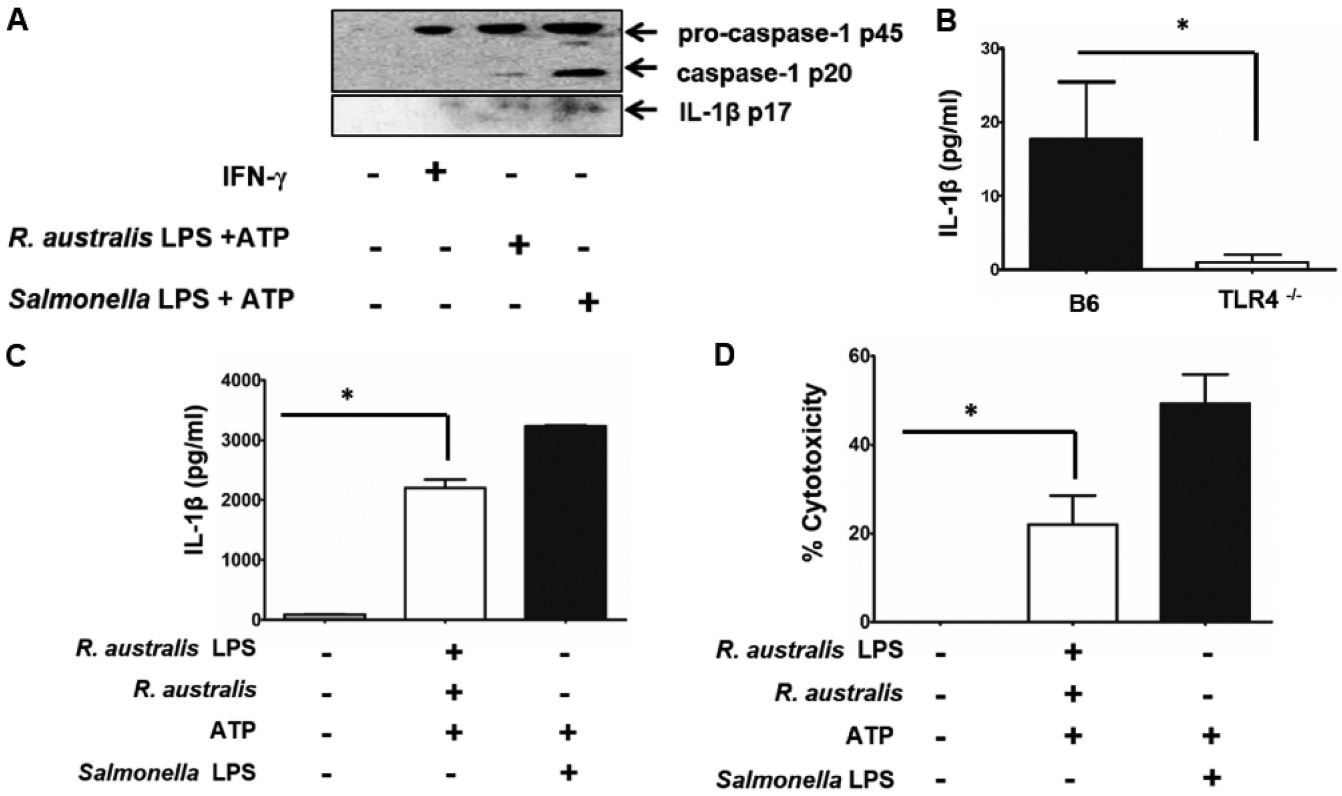

FIG 6 Rickettsial LPS serves as an efficient stimulus for activating inflammasome in macrophages. Rickettsial LPS was isolated and purified. BMMs were isolated from B6 and TLR4$^{-/-}$ mice. Rickettsial LPS was added to BMMs at a concentration of 100 ng/ml for 24 h. ATP (5 mM) was added to the cell culture for 1 h prior to collection. *Salmonella* LPS (100 ng/ml) plus ATP served as the positive control. (A) Supernatants of B6 BMMs stimulated with rickettsial LPS and ATP were collected and then concentrated. Activation of inflammasome was evaluated by immunoblotting using specific antibodies against pro-caspase-1 (p45), activated caspase-1 (p20), and activated IL-1β (p17). BMMs stimulated with IFN-γ (40 ng/ml) served as controls. (B) Supernatants of BMMs from B6 and TLR4$^{-/-}$ mice stimulated with purified LPS of *R. australis* and ATP were collected. Secretion levels of IL-1β by these stimulated cells were measured by ELISA. Next, B6 BMMs were first primed with 100 ng/ml rickettsial LPS and then infected with *R. australis* at an MOI of 6. Then, 5 mM ATP was added to the cells for 1 h prior to collection of the supernatant. Secretion levels of IL-1β was determined by ELISA (C). The cytotoxicity was determined by LDH assay (D). Data represent two independent experiments. *, $P < 0.05$.

LPS and ATP stimulation in combination with *R. australis* infection led to significant production of IL-1β by B6 BMMs, but at a lower level than *Salmonella* LPS and ATP. The level of IL-1β secretion by BMMs stimulated by *R. australis* LPS plus ATP (Fig. 6B) was much lower than levels stimulated by *R. australis* LPS followed by *R. australis* infection plus ATP (Fig. 6C), suggesting that an LPS-independent ligand in rickettsiae also contributes to inflammasome activation. To investigate whether cytotoxicity is induced by these stimulations, we determined cytotoxicity by LDH release. As shown in Fig. 6D, we found around 20% of cytotoxicity upon priming by *R. australis* LPS followed by infection with *R. australis* and stimulating with ATP. We did not find a significant level of cytotoxicity in *R. australis*-infected BMMs. These results suggest that rickettsial LPS stimulation leads to the transcriptional upregulation and subsequent translation of pro-IL-1β and that rickettsial LPS acts as a priming signal for inflammasome activation in a TLR4-dependent manner.

DISCUSSION

We previously demonstrated that *R. australis* activates ASC-dependent inflammasome in both human and mouse macrophages, as evidenced by cleavage of pro-caspase-1 and pro-IL-1β and secretion of inflammasome-dependent cytokines, including IL-1β and/or IL-18 (5). The previous and present studies dissected the host and microbial signals involved in the activation of inflammasome by *R. australis*, as shown in Fig. 7. *R. australis* is sensed by TLR4-ASC inflammasome in macrophages, leading to antirickettsial inflammatory responses in which IL-1β serves as a major

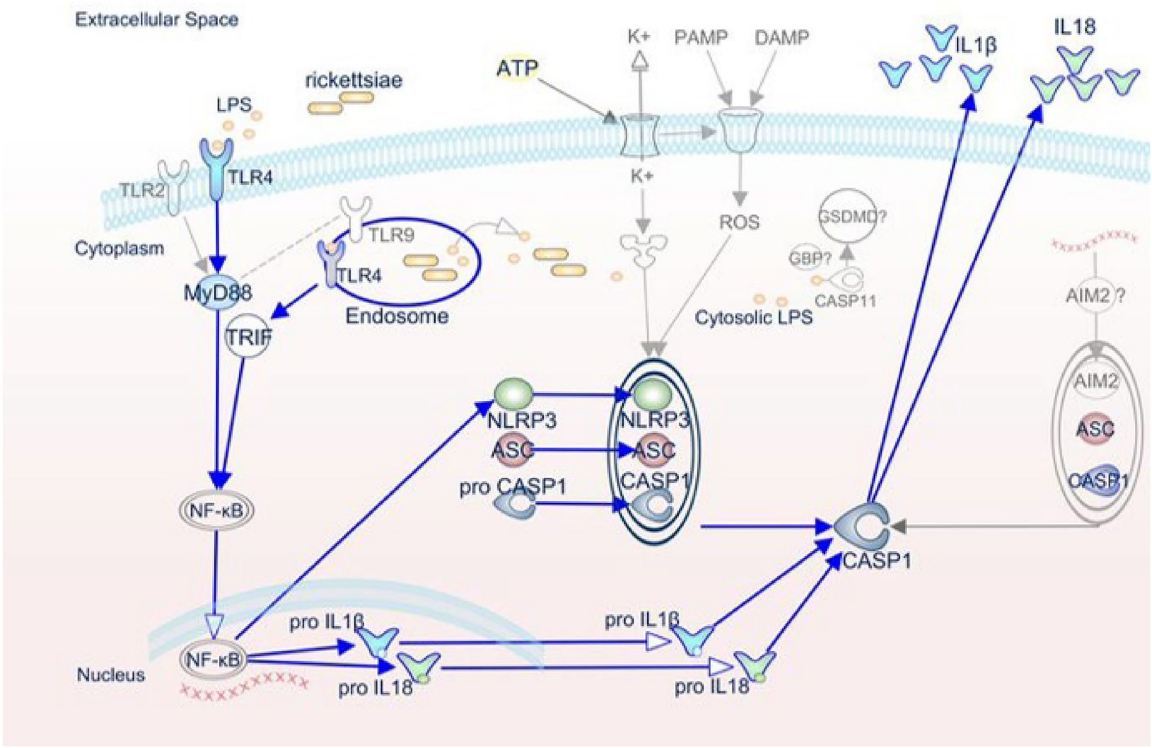

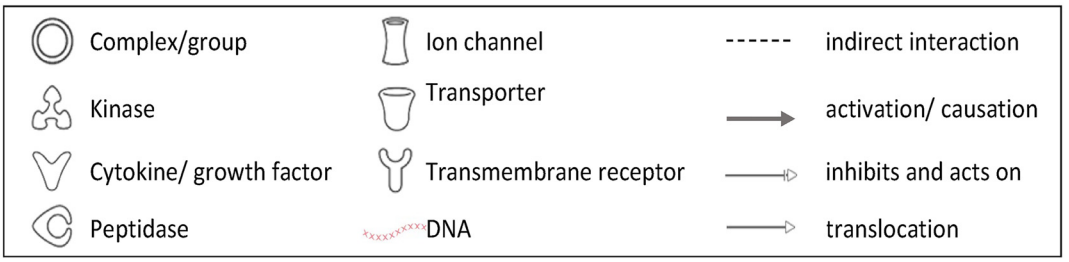

FIG 7 Schematic diagram of inflammasome activation by rickettsiae. This IPA-generated schematic depicts the molecular mechanisms involved in the activation of inflammasome by pathogen-associated molecular patterns during rickettsial infection. *R. australis* is recognized by and triggers the host's NLRP3/ASC inflammasome, which leads to caspase-1 activation and secretion of IL-1β and IL-18 and culminates in the control of bacterial replication in macrophages and *in vivo*. In murine macrophages, whereas NLRP3 is dispensable for inflammasome activation by *R. australis*, AIM2/ASC is hypothesized to play a role. The priming signal for NLRP3 inflammasome activation is provided by recognition of rickettsial LPS by host TLR4 in both MyD88-dependent and -independent mechanisms. Rickettsiae invade the host cytosol to provide signal 2 for NLRP3/ASC inflammasome through an unknown molecule. Pathways demonstrated in our studies are blue, while mechanisms hypothesized but not tested are gray.

player. Recognition of rickettsial LPS by host TLR4 provides the priming signal for the activation of ASC–caspase-1–IL-1β inflammasome during rickettsial infection. We further demonstrated that ASC inflammasome plays an important role in host control of rickettsiae *in vivo* by using a mouse model of spotted fever rickettsioses.

TLR4 is one of the essential elements of host protective immunity against rickettsiae. TLR4 deficiency leads to compromise of immune responses in animal models of rickettsial infections in association with significantly reduced production of IFN-γ by both NK cells and Th1 cells (14, 16). In line with these results, TLR4$^{-/-}$ BMMs in our studies contained greater concentrations of intracellular *R. australis* than B6 BMMs, suggesting that TLR4 contributes to host protection against rickettsiae also by mediating rickettsial clearance in macrophages. Our recent studies showed the importance of MyD88 in mediating protective inflammatory responses to rickettsiae (17). While those studies focused on DC, the present study showed that MyD88 contributed to

IL-1β secretion by *R. australis*-infected BMMs. In response to *R. australis* infection, the secretion of IL-1β was completely abrogated by a TLR4 deficiency and was significantly reduced by a MyD88 deficiency compared to that in B6 BMMs. These results suggest that MyD88-independent signals are also involved in regulating TLR4-ASC-dependent IL-1β secretion during rickettsial infection. MyD88 is an adaptor for multiple TLRs, including TLR4. However, TLR4 can also signal through Toll/IL-1R domain–containing adaptor-inducing IFN-β (TRIF). It has been reported that TLR4-TRIF signaling occurs from the endosome, whereas TLR4-MyD88 signaling is initiated from the plasma membrane (25). Thus, we propose that *R. australis* activates TLR4 signals through both MyD88 at the cell-surface and TRIF from the endosomes (Fig. 7). Although the secretion of IL-1β was completely TLR4 dependent, the expression level of pro-IL-1β was only partially reduced in TLR4$^{-/-}$ BMMs compared to B6 BMMs upon rickettsial infection. The possible interpretations for this observation are (i) that the level of pro-IL-1β in TLR4$^{-/-}$ BMMs is too low to lead to detectable level of IL-1β secretion and (ii) that TLR4 is involved in the second signal of inflammasome activation. Thus, our results highlighted the idea that the LPS-TLR4 interactions provide the priming signal for biosynthesis of pro-IL-1β, which is subsequently cleaved by the active caspase-1 in *R. australis*-infected mouse macrophages.

IL-1β is one of the most potent IL-1 family cytokines. Protection provided by IL-1β in infectious disease models is mainly associated with the ability of IL-1β to induce a rapid neutrophil response and induction of chemokines and cytokines (26). IL-1β plays a role in killing of bacteria, including *Pseudomonas aeruginosa* (27) and *Mycobacterium tuberculosis* (28). Jayaraman et al. (28) have shown that IL-1β kills *M. tuberculosis* by upregulating TNF receptor and caspase-3 activation. Interestingly, we found that IL-1β stimulated a rickettsicidal response in macrophages. Accordingly, we recently reported that elevated IL-1β may account for reduced loads of *R. australis* in *Atg5*-deficient macrophages (11). In human infection, IL-1β is detectable in the serum of patients with the Israeli spotted fever strain of *R. conorii* at the early phase of infection (29). Feng and Walker demonstrated that endothelium can kill intracellular pathogens via nitric oxide (23). Further studies are required to reveal the mechanisms by which IL-1β drives rickettsial killing in macrophages.

Our studies demonstrated the contribution of ASC inflammasome to host protective immunity against rickettsiae is in association with enhanced *in vivo* production of IL-1β, IL-18, and IFN-γ. IFN-γ is a key effector in host control of rickettsial infection (21, 30). Given the low level of IL-1 receptors on NK cells and the relatively less important role of IL-1β in priming NK cells, it is unlikely that IL-1β deficiency alone results in decreased IFN-γ production. The protective effects of IL-18 in infectious disease models mainly result from the ability of IL-18 to stimulate secretion of IFN-γ from both NK and T cells (31) and to amplify the cytotoxicity of CD8$^+$ T cells and NK cells (26, 32). IL-18-mediated protection has been reported in several infection models, including anaplasmosis and *Burkholderia pseudomallei* infection (33, 34). Pedra et al. reported that IL-18$^{-/-}$ mice show the same level of mortality as ASC$^{-/-}$ mice in a model of anaplasmosis, due to the lack of activation of NK cells and the subsequent lack of IFN-γ (33). Thus, in addition to IL-1β, IL-18 is also possibly involved in ASC inflammasome-mediated protective immunity against rickettsial diseases. Given the downstream importance of ASC in host defense, more studies are justified to fully investigate the repercussions of this inflammasome adaptor protein.

In our studies, purified LPS from *R. australis* resulted in a TLR4-dependent level of IL-1β secretion in macrophages. The nature of the interaction of rickettsial LPS with host mammalian cells remains largely unknown. LPS in rickettsiae was initially identified as a group-specific antigen among the pathogenic spotted fever and typhus groups of rickettsiae (35, 36). Due to the lower levels of LPS in rickettsiae, 1 to 2% of rickettsial biomass (37), it has been challenging to study the LPS of rickettsiae, specifically with regard to isolating the LPS, characterizing its biological properties, and correlating the *in vitro* findings with the *in vivo* pathophysiological significance. Recent studies have reported that the alternative lipid A acyltransferase from *Rickettsia* catalyzes the addi-

tion of C_{16} fatty acid chains into the lipid A 3′-linked primary acyl chain, accounting for major structural differences relative to the highly inflammatory lipid A of *Escherichia coli* (4, 38). Little is known about whether rickettsial LPS acts as a TLR4 agonist and/or is associated with caspase-11-dependent noncanonical inflammasome. Our results suggest that rickettsial LPS can serve as a PAMP to be recognized by TLR4 in macrophages, which subsequently acts as the priming signal for activation of ASC inflammasome. The noncanonical inflammasome has been recently considered a key player that promotes host surveillance during cytosolic infection with Gram-negative bacteria (9). The current data cannot exclude the possibility that cytosolic rickettsial LPS may directly activate noncanonical inflammasome. More structural data and mechanistic studies may advance the field of knowledge of the contribution of rickettsial LPS to evasion of the host immune system.

In conclusion, our study demonstrated that *R. australis* activated the ASC–caspase-1–IL-1β inflammasome cascade in macrophages, most likely through TLR4 by its LPS. ASC inflammasome is required for host protective immune responses against rickettsial diseases in association with enhanced *in vivo* bacterial clearance and production of inflammasome-dependent proinflammatory and effector cytokines.

MATERIALS AND METHODS

***Rickettsia* and mice.** *Rickettsia australis* (Cutlack strain) organisms used for animal inoculation were propagated in pathogen-free embryonated chicken eggs as described previously (39). For *in vitro* macrophage infection, *R. australis* (Cutlack strain) was cultivated in Vero cells and purified as previously described with modifications (11, 40). Briefly, infected cells were placed on the top of 32%, 26%, and 20% OptiPrep density gradient medium in a 6× SPG buffer (218 mM sucrose, 3.76 mM KH_2PO_4, 7.1 mM K_2HPO_4, 4.9 mM potassium glutamate) bed (Sigma-Aldrich, St. Louis, MO) after sonication. All rickettsial stocks were quantified by plaque assay and stored at −80°C until use. B6 mice and TLR4$^{-/-}$ mice were purchased from Jackson Laboratories (Bar Harbor, ME). ASC$^{-/-}$ mice were kindly provided by Vishva Dixit at Genentech, Inc. (South San Francisco, CA). For *in vivo* experiments, mice were inoculated intravenously (i.v.) through the tail vein with *R. australis* at the doses indicated in the figure legends. After infection, mice were monitored daily for signs of illness until day 20 p.i. To determine the bacterial loads in tissues and immune response *in vivo*, mice were sacrificed on day 4 p.i. All the experiments described in this study were performed in a certified biosafety level 3 (BSL3) laboratory at the University of Texas Medical Branch (UTMB). All mice were maintained and manipulated in an animal BSL3 facility at UTMB. The UTMB Animal Care and Use Committee approved all experiments and procedures, and experiments with mice were performed according to the guidelines of the *Guide for the Care and Use of Laboratory Animals* (41).

Generation of BMMs. The generation of primary BMMs from 6- to 8-week-old B6, TLR4$^{-/-}$, ASC$^{-/-}$, and MyD88$^{-/-}$ mice was performed as previously described (5). Briefly, after the femurs and tibias were dissected, the bone marrow was flushed, and cells were cultivated in low-endotoxin Dulbecco modified Eagle medium (DMEM) containing 10% (vol/vol) newborn calf serum (Gibco, Thermo Fisher Scientific) supplemented with either 20% supernatant from an L929 cell culture or a CMG14-12 cell culture or recombinant macrophage colony-stimulating factor (PeproTech) at 37°C in 5% CO_2 (42). On day 6 of culture, cells were harvested and characterized by flow-cytometric analysis after staining with anti-F4/80 and anti-CD11b antibodies (Abs) (catalog numbers 565410 and 553310; BD Bioscience). In some experiments, the bone marrow cells were seeded into 100-mm non-tissue culture-treated petri dishes (Fisher Scientific) at 1×10^6 cells/ml in DMEM (Gibco) and supplemented to final concentrations of 20% fetal bovine serum, 10 ng/ml mouse IL-3 (Peprotech), 10 ng/ml mouse IL-6 (Peprotech), and 50 ng/ml mouse stem cell factor (Peprotech) in BMM medium. Cells were incubated as described above and allowed to expand for 3 to 5 days. Once confluent, cells were centrifuged at 300 × *g* for 5 min and replated in BMM medium for differentiation into BMMs. More than approximately 85% of these cells were F4/80$^+$ and CD11b$^+$ (see Fig. S1 in the supplemental material). These cells were plated in 24-well plates at a density of 1×10^6 cells/well and used for experiments after overnight incubation.

Macrophage *in vitro* infections or stimulations. BMMs and RAW 264.7 cells were infected with purified *R. australis* at a multiplicity of infection (MOI) of 6 or 2 (see the figure legends). Rickettsiae were centrifuged onto the cells at 560 × *g* for 5 min. For some experiments, cells were stimulated with 50 or 100 ng/ml of purified *R. australis* LPS and 5 mM ATP (Invivogen). ATP was added to the cell culture for 1 h prior to collection. Cells were incubated at 37°C in 5% CO_2. At 24 h p.i. or poststimulation, supernatant was collected and filtered with 0.22-μm syringe-driven filter units (EMD Millipore, Burlington, MA), and cells were collected and washed for further experiments. Uninfected macrophages served as negative controls. BMMs stimulated with 100 ng/ml of purified *Salmonella enterica* serovar Minnesota LPS (List Biologicals Laboratories) and 5 mM ATP (Invivogen) served as positive controls.

Western blotting. For assessment of the cellular expression levels of different inflammasome components, including pro-caspase-1, active caspase-1, pro-IL-1β, active IL-1β, and β-actin, cells were lysed with radioimmunoprecipitation assay (RIPA) lysis buffer (EMD Millipore, Burlington, MA) supplemented with protease inhibitors (Roche, Indianapolis, IN). The soluble part of cell lysates was isolated by centrifugation and used for immunoblotting. Cell culture supernatants were processed in centrifugal filter units (3K; Amicon) according to the instructions of the manufacturer. Briefly, 2 ml of supernatant

were loaded onto columns and centrifuged at 7,000 × *g* for 60 min at 4°C. Protein concentration was determined by bicinchoninic acid assay (Pierce). Both cell lysates and concentrated cell culture supernatants were separated by sodium dodecyl sulfate-polyacrylamide gel electrophoresis, transferred to polyvinylidene difluoride membranes, and probed with a rabbit polyclonal Ab directed against pro-IL-1β and active IL-1β (clone D3H1Z, catalog number 12507; Cell Signaling) at a dilution of 1:1,000 and pro-caspase-1 at a dilution of 1:500 (catalog number 06-503-I; EMD Millipore, Burlington, MA) for lysates and against active caspase-1 at a dilution of 1:100 (NBP1-45433; Novus Biologicals) for concentrated supernatants. Immunoreactive bands were visualized using an appropriate secondary Ab and enhanced chemiluminescence detection reagents (Thermo Scientific, Pierce, IL). Equal protein loading of the gels was controlled by detecting β-actin with mouse monoclonal Ab (catalog number A1978; Sigma, St. Louis, MO) in the cellular lysates.

Quantification of bacterial loads by quantitative real-time PCR. To determine the number of intracellular rickettsiae following *in vitro* macrophage infection, *R. australis*-infected BMMs or RAW 267.4 cells were collected at different time intervals p.i. as described above, and DNA was extracted from these cells using a DNA extraction kit (Qiagen, Valencia, CA) as described previously (40). Mouse lungs, livers, and spleens were collected in RNAlater (Thermo Fisher Scientific, Waltham, MA). Rickettsial loads in the mouse tissues were quantified using quantitative PCR following DNA extraction as described previously (30). Quantitative real-time PCR was performed using the iCycler from Bio-Rad (Hercules, CA). Rickettsial loads were determined by real-time PCR with primers and TaqMan probes for the *Rickettsia*-specific citrate synthase (CS) gene (*gltA*) as described in our previous studies: *gltA* forward, GAGAGAAAATTATA TCCAAATGTTGAT; *gltA* reverse, AGGGTCTTCGTGCATTTCTT; *gltA* probe, CATTGTGCCATCCAGCCTACGGT. The *gltA* probe was labeled with 6-carboxyfluorescein (FAM) and Black Hole Quencher 1 (Biosearch Technologies, Petaluma, CA). Two-step cycle parameters (95°C and 60°C) were used. The results were normalized to the amount (in nanograms) of genomic DNA in the same sample and expressed as CS copy number per nanogram of genomic DNA.

Histopathological analyses. Formalin-fixed, hematoxylin and eosin (H&E)-stained tissue sections from infected and uninfected mice were evaluated by a pathologist via both low-magnification (×10) and high-magnification (×40) microscopy. Images were taken using an Olympus BX41 photomicroscope (Olympus America, Inc., Center Valley, PA).

Extraction and quantification of *R. australis* LPS. *Rickettsia australis* was propagated in Vero cells and purified as described previously (11, 30). Briefly, infected cells were collected and suspended in SPG buffer after sonication. Rickettsiae were placed on top of a 20% Optiprep density gradient in 1× SPG buffer after sonication. After centrifugation, rickettsiae were washed with 1× SPG and collected. Rickettsiae were killed by exposure to 90°C for 2 h in a certified biosafety level 3 (BSL3) laboratory. Rickettsiae were then treated with 100 μg/ml of proteinase K for 16 h at 37°C. The resulting lysate was centrifuged at 12,000 × *g* for 30 min at 4°C. The pellet was processed using an LPS purification kit (Intron Biotechnology, Gyeonggi-do, South Korea) (43–45). Briefly, lysis buffer was added to the rickettsial pellet, and the mixture was vortexed until homogenous. Chloroform was added, and the mixture was vortexed again and then incubated at room temperature for 5 min. The mixture was centrifuged at 13,200 × *g* for 10 min at 4°C, and 400 μl of supernatant was transferred into a new tube. The supernatant was centrifuged again and then washed with 1 ml of 70% ethanol. The pellet was resuspended in 10 mM Tris-HCl buffer and boiled for 1 min. Next, rickettsial LPS was visualized and quantified via silver staining using known concentrations of *E. coli* LPS (List Biologicals Laboratories) as a standard for quantification.

Cytokine ELISA. Filtered supernatants of BMMs or sera treated with 0.9% sodium azide were collected for inactivating live *R. australis* in order to transfer the specimen from the BSL3 laboratory to a BSL2 laboratory. IL-10, IFN-γ, IL-1β, and IL-18 concentrations were measured by using Quantikine ELISA kits (R&D Systems, Minneapolis, MN). Absorbance was measured using the VersaMax microplate reader (Molecular Devices, Sunnyvale, CA). The limits of detection of the ELISA for cytokine measurements were as follows: IL-1β, 1.0 pg/ml; IL-10, 5.22 pg/ml; IFN-γ, 2 pg/ml; and IL-18, 25 pg/ml.

LDH cytotoxicity assay. A CytoTox96 nonradioactive cytotoxicity assay (Promega) was used to measure percent cytotoxicity, according to the manufacturer's instructions as described previously (46, 47). Briefly, supernatants were collected from macrophages after stimulation with rickettsial LPS followed by *R. australis* infection for 24 h and ATP treatment. Lysis buffer (10×) was added to the wells and diluted to a 1× final concentration in medium. The cells were incubated for 45 min at 37°C to lyse the cells. The 24-well plate was centrifuged for 4 min at 560 × *g*, and medium was then collected for total-lactate dehydrogenase (LDH) determination. Assay buffer (12 ml) was mixed with one vial of assay substrate, and 50 μl of supernatant or 50 μl of lysate was placed in a 96-well plate and mixed with 50 μl of the assay substrate. The plate was incubated for 15 min while protected from light, and 50 μl of stop solution was added to each well. The absorbances of the wells were read at 490 nm using the VersaMax microplate reader (Molecular Devices, Sunnyvale, CA). Cell death was calculated as the ratio of LDH activity in the supernatant alone to the maximum LDH activity of lysed cells.

Statistical analysis. For comparison of multiple experimental groups, one-way analysis of variance (ANOVA) with Bonferroni's procedure was used. Two-group comparison was conducted using either Student's *t* test or Welch's *t* test, depending on whether the variance between two groups was significantly different. To determine whether the difference in survival between different mouse groups was significant, data were analyzed by the Gehan-Breslow-Wilcoxon test. All the statistical analyses were performed using GraphPad Prism software, version 5.01. *P* values of 0.05 or less were the threshold for statistical significance.

Pathway Designer graphical representation. The schematic representation of pathogen-induced priming and activation mechanism of the inflammasome was generated through the use

of Ingenuity Pathway Analysis (IPA) (http://qiagen.force.com/KnowledgeBase/KnowledgeIPAPage?id=kA1D0000000PIpmKAG). The inflammasome pathway was selected from the eligible pathways in the IPA library, which summarizes several inflammasome complexes based on references from the literature, from textbooks, or from canonical information stored in the Ingenuity Pathways Knowledge Base (48). Pathway Designer function was then utilized to further customize the schematic model to summarize the findings.

SUPPLEMENTAL MATERIAL

Supplemental material is available online only.

SUPPLEMENTAL FILE 1, PDF file, 0.01 MB.

ACKNOWLEDGMENTS

We thank Vishva Dixit for his generous gift of breeding pairs of $ASC^{-/-}$ mice. Edward A. Miao at the University of North Carolina at Chapel Hill and Joao Pedra at the University of Maryland School of Medicine provided very insightful discussions on inflammasomes. Tais Saito provided technical assistance with isolating mouse organs. Donald H. Bouyer and Nicole L. Mendell provided assistance with taking the images for histopathological analysis.

This work was supported by grant AI133359 to R.F. from the National Institute of Allergy and Infectious Diseases. C.R. was supported by the National Institutes of Health T32 Training Grant (AI060549) at the University of Texas Medical Branch.

We declare that there is no conflict of interest.

REFERENCES

1. Binder AM, Nichols Heitman K, Drexler NA. 2019. Diagnostic methods used to classify confirmed and probable cases of spotted fever rickettsioses—United States, 2010–2015. MMWR Morb Mortal Wkly Rep 68:243–246. https://doi.org/10.15585/mmwr.mm6810a3.
2. Drexler NA, Yaglom H, Casal M, Fierro M, Kriner P, Murphy B, Kjemtrup A, Paddock CD. 2017. Fatal Rocky Mountain spotted fever along the United States-Mexico Border, 2013–2016. Emerg Infect Dis 23:1621–1626. https://doi.org/10.3201/eid2310.170309.
3. Takeuchi O, Akira S. 2010. Pattern recognition receptors and inflammation. Cell 140:805–820. https://doi.org/10.1016/j.cell.2010.01.022.
4. Guillotte ML, Gillespie JJ, Chandler CE, Rahman MS, Ernst RK, Azad AF. 2018. *Rickettsia* lipid A biosynthesis utilizes the late acyltransferase LpxJ for secondary fatty acid addition. J Bacteriol 200:e00334-18. https://doi.org/10.1128/JB.00334-18.
5. Smalley C, Bechelli J, Rockx-Brouwer D, Saito T, Azar SR, Ismail N, Walker DH, Fang R. 2016. *Rickettsia australis* activates inflammasome in human and murine macrophages. PLoS One 11:e0157231. https://doi.org/10.1371/journal.pone.0157231.
6. Yang Y, Wang H, Kouadir M, Song H, Shi F. 2019. Recent advances in the mechanisms of NLRP3 inflammasome activation and its inhibitors. Cell Death Dis 10:128. https://doi.org/10.1038/s41419-019-1413-8.
7. Han S, Lear TB, Jerome JA, Rajbhandari S, Snavely CA, Gulick DL, Gibson KF, Zou C, Chen BB, Mallampalli RK. 2015. Lipopolysaccharide primes the NALP3 inflammasome by inhibiting its ubiquitination and degradation mediated by the SCFFBXL2 E3 ligase. J Biol Chem 290:18124–18133. https://doi.org/10.1074/jbc.M115.645549.
8. Gaidt MM, Hornung V. 2017. Alternative inflammasome activation enables IL-1beta release from living cells. Curr Opin Immunol 44:7–13. https://doi.org/10.1016/j.coi.2016.10.007.
9. Gomes MTR, Cerqueira DM, Guimaraes ES, Campos PC, Oliveira SC. 2019. Guanylate-binding proteins at the crossroad of noncanonical inflammasome activation during bacterial infections. J Leukoc Biol 106:553–562. https://doi.org/10.1002/JLB.4MR0119-013R.
10. Baker PJ, Boucher D, Bierschenk D, Tebartz C, Whitney PG, D'Silva DB, Tanzer MC, Monteleone M, Robertson AAB, Cooper MA, Alvarez-Diaz S, Herold MJ, Bedoui S, Schroder K, Masters SL. 2015. NLRP3 inflammasome activation downstream of cytoplasmic LPS recognition by both caspase-4 and caspase-5. Eur J Immunol 45:2918–2926. https://doi.org/10.1002/eji.201545655.
11. Bechelli J, Vergara L, Smalley C, Buzhdygan TP, Bender S, Zhang W, Liu Y, Popov VL, Wang J, Garg N, Hwang S, Walker DH, Fang R. 2019. *Atg5* supports *Rickettsia australis* infection in macrophages *in vitro* and *in vivo*. Infect Immun 87:e00651-18. https://doi.org/10.1128/IAI.00651-18.
12. Cragun WC, Bartlett BL, Ellis MW, Hoover AZ, Tyring SK, Mendoza N, Vento TJ, Nicholson WL, Eremeeva ME, Olano JP, Rapini RP, Paddock CD. 2010. The expanding spectrum of eschar-associated rickettsioses in the United States. Arch Dermatol 146:641–648. https://doi.org/10.1001/archdermatol.2010.48.
13. Walker DH, Hudnall SD, Szaniawski WK, Feng HM. 1999. Monoclonal antibody-based immunohistochemical diagnosis of rickettsialpox: the macrophage is the principal target. Mod Pathol 12:529–533.
14. Jordan JM, Woods ME, Soong L, Walker DH. 2009. Rickettsiae stimulate dendritic cells through Toll-like receptor 4, leading to enhanced NK cell activation *in vivo*. J Infect Dis 199:236–242. https://doi.org/10.1086/595833.
15. Jordan JM, Woods ME, Feng HM, Soong L, Walker DH. 2007. Rickettsiae-stimulated dendritic cells mediate protection against lethal rickettsial challenge in an animal model of spotted fever rickettsiosis. J Infect Dis 196:629–638. https://doi.org/10.1086/519686.
16. Jordan JM, Woods ME, Olano J, Walker DH. 2008. The absence of Toll-like receptor 4 signaling in C3H/HeJ mice predisposes them to overwhelming rickettsial infection and decreased protective Th1 responses. Infect Immun 76:3717–3724. https://doi.org/10.1128/IAI.00311-08.
17. Bechelli J, Smalley C, Zhao X, Judy B, Valdes P, Walker DH, Fang R. 2016. MyD88 mediates instructive signaling in dendritic cells and protective inflammatory response during rickettsial infection. Infect Immun 84:883–893. https://doi.org/10.1128/IAI.01361-15.
18. Feng HM, Wen J, Walker DH. 1993. *Rickettsia australis* infection: a murine model of a highly invasive vasculopathic rickettsiosis. Am J Pathol 142:1471–1482.
19. Xin L, Shelite TR, Gong B, Mendell NL, Soong L, Fang R, Walker DH. 2012. Systemic treatment with CpG-B after sublethal rickettsial infection induces mouse death through indoleamine 2,3-dioxygenase (IDO). PLoS One 7:e34062. https://doi.org/10.1371/journal.pone.0034062.
20. Walker DH, Olano JP, Feng HM. 2001. Critical role of cytotoxic T lymphocytes in immune clearance of rickettsial infection. Infect Immun 69:1841–1846. https://doi.org/10.1128/IAI.69.3.1841-1846.2001.
21. Feng HM, Popov VL, Walker DH. 1994. Depletion of gamma interferon and tumor necrosis factor alpha in mice with *Rickettsia conorii*-infected endothelium: impairment of rickettsicidal nitric oxide production resulting in fatal, overwhelming rickettsial disease. Infect Immun 62:1952–1960. https://doi.org/10.1128/IAI.62.5.1952-1960.1994.
22. Feng H, Popov VL, Yuoh G, Walker DH. 1997. Role of T lymphocyte subsets in immunity to spotted fever group rickettsiae. J Immunol 158:5314–5320.
23. Feng HM, Walker DH. 2000. Mechanisms of intracellular killing of *Rick-*

ettsia conorii in infected human endothelial cells, hepatocytes, and macrophages. Infect Immun 68:6729–6736. https://doi.org/10.1128/iai.68.12.6729-6736.2000.
24. Stammler D, Eigenbrod T, Menz S, Frick JS, Sweet MJ, Shakespear MR, Jantsch J, Siegert I, Wolfle S, Langer JD, Oehme I, Schaefer L, Fischer A, Knievel J, Heeg K, Dalpke AH, Bode KA. 2015. Inhibition of histone deacetylases permits lipopolysaccharide-mediated secretion of bioactive IL-1beta via a caspase-1-independent mechanism. J Immunol 195:5421–5431. https://doi.org/10.4049/jimmunol.1501195.
25. Cheng Z, Taylor B, Ourthiague DR, Hoffmann A. 2015. Distinct single-cell signaling characteristics are conferred by the MyD88 and TRIF pathways during TLR4 activation. Sci Signal 8:ra69. https://doi.org/10.1126/scisignal.aaa5208.
26. Sahoo M, Ceballos-Olvera I, del Barrio L, Re F. 2011. Role of the inflammasome, IL-1beta, and IL-18 in bacterial infections. ScientificWorldJournal 11:2037–2050. https://doi.org/10.1100/2011/212680.
27. Descamps D, Le Gars M, Balloy V, Barbier D, Maschalidi S, Tohme M, Chignard M, Ramphal R, Manoury B, Sallenave JM. 2012. Toll-like receptor 5 (TLR5), IL-1beta secretion, and asparagine endopeptidase are critical factors for alveolar macrophage phagocytosis and bacterial killing. Proc Natl Acad Sci U S A 109:1619–1624. https://doi.org/10.1073/pnas.1108464109.
28. Jayaraman P, Sada-Ovalle I, Nishimura T, Anderson AC, Kuchroo VK, Remold HG, Behar SM. 2013. IL-1beta promotes antimicrobial immunity in macrophages by regulating TNFR signaling and caspase-3 activation. J Immunol 190:4196–4204. https://doi.org/10.4049/jimmunol.1202688.
29. Parola P, Paddock CD, Socolovschi C, Labruna MB, Mediannikov O, Kernif T, Abdad MY, Stenos J, Bitam I, Fournier PE, Raoult D. 2013. Update on tick-borne rickettsioses around the world: a geographic approach. Clin Microbiol Rev 26:657–702. https://doi.org/10.1128/CMR.00032-13.
30. Fang R, Ismail N, Walker DH. 2012. Contribution of NK cells to the innate phase of host protection against an intracellular bacterium targeting systemic endothelium. Am J Pathol 181:185–195. https://doi.org/10.1016/j.ajpath.2012.03.020.
31. Dinarello CA, Fantuzzi G. 2003. Interleukin-18 and host defense against infection. J Infect Dis 187(Suppl 2):S370–S384. https://doi.org/10.1086/374751.
32. Tewari K, Nakayama Y, Suresh M. 2007. Role of direct effects of IFN-gamma on T cells in the regulation of CD8 T cell homeostasis. J Immunol 179:2115–2125. https://doi.org/10.4049/jimmunol.179.4.2115.
33. Pedra JH, Tao J, Sutterwala FS, Sukumaran B, Berliner N, Bockenstedt LK, Flavell RA, Yin Z, Fikrig E. 2007. IL-12/23p40-dependent clearance of *Anaplasma phagocytophilum* in the murine model of human anaplasmosis. FEMS Immunol Med Microbiol 50:401–410. https://doi.org/10.1111/j.1574-695X.2007.00270.x.
34. Wiersinga WJ, Wieland CW, van der Windt GJ, de Boer A, Florquin S, Dondorp A, Day NP, Peacock SJ, van der Poll T. 2007. Endogenous interleukin-18 improves the early antimicrobial host response in severe melioidosis. Infect Immun 75:3739–3746. https://doi.org/10.1128/IAI.00080-07.
35. Vishwanath S. 1991. Antigenic relationships among the rickettsiae of the spotted fever and typhus groups. FEMS Microbiol Lett 65:341–344. https://doi.org/10.1016/0378-1097(91)90238-6.
36. Amano KI, Williams JC, Dasch GA. 1998. Structural properties of lipopolysaccharides from *Rickettsia typhi* and *Rickettsia prowazekii* and their chemical similarity to the lipopolysaccharide from *Proteus vulgaris* OX19 used in the Weil-Felix test. Infect Immun 66:923–926. https://doi.org/10.1128/IAI.66.3.923-926.1998.
37. Fodorova M, Vadovic P, Skultety L, Slaba K, Toman R. 2005. Structural features of lipopolysaccharide from *Rickettsia typhi*: the causative agent of endemic typhus. Ann N Y Acad Sci 1063:259–260. https://doi.org/10.1196/annals.1355.041.
38. Fodorova M, Vadovic P, Toman R. 2011. Structural features of lipid A of *Rickettsia typhi*. Acta Virol 55:31–44. https://doi.org/10.4149/av_2011_01_31.
39. Fang R, Ismail N, Shelite T, Walker DH. 2009. $CD4^+$ $CD25^+$ $Foxp3^-$ T-regulatory cells produce both gamma interferon and interleukin-10 during acute severe murine spotted fever rickettsiosis. Infect Immun 77:3838–3849. https://doi.org/10.1128/IAI.00349-09.
40. Fang R, Ismail N, Soong L, Popov VL, Whitworth T, Bouyer DH, Walker DH. 2007. Differential interaction of dendritic cells with *Rickettsia conorii*: impact on host susceptibility to murine spotted fever rickettsiosis. Infect Immun 75:3112–3123. https://doi.org/10.1128/IAI.00007-07.
41. National Research Council. 2011. Guide for the care and use of laboratory animals, 8th ed. National Academies Press, Washington, DC.
42. Takeshita S, Kaji K, Kudo A. 2000. Identification and characterization of the new osteoclast progenitor with macrophage phenotypes being able to differentiate into mature osteoclasts. J Bone Miner Res 15:1477–1488. https://doi.org/10.1359/jbmr.2000.15.8.1477.
43. Lee SH, Kim KK, Rhyu IC, Koh S, Lee DS, Choi BK. 2006. Phenol/water extract of *Treponema socranskii* subsp. *socranskii* as an antagonist of Toll-like receptor 4 signalling. Microbiology 152:535–546. https://doi.org/10.1099/mic.0.28470-0.
44. Paramonov NA, Aduse-Opoku J, Hashim A, Rangarajan M, Curtis MA. 2009. Structural analysis of the core region of O-lipopolysaccharide of *Porphyromonas gingivalis* from mutants defective in O-antigen ligase and O-antigen polymerase. J Bacteriol 191:5272–5282. https://doi.org/10.1128/JB.00019-09.
45. Nualnoi T, Norris MH, Tuanyok A, Brett PJ, Burtnick MN, Keim PS, Settles EW, Allender CJ, AuCoin DP. 2017. Development of immunoassays for *Burkholderia pseudomallei* typical and atypical lipopolysaccharide strain typing. Am J Trop Med Hyg 96:358–367. https://doi.org/10.4269/ajtmh.16-0308.
46. Rayamajhi M, Zhang Y, Miao EA. 2013. Detection of pyroptosis by measuring released lactate dehydrogenase activity. Methods Mol Biol 1040:85–90. https://doi.org/10.1007/978-1-62703-523-1_7.
47. Rapsinski GJ, Wynosky-Dolfi MA, Oppong GO, Tursi SA, Wilson RP, Brodsky IE, Tükel Ç. 2015. Toll-like receptor 2 and NLRP3 cooperate to recognize a functional bacterial amyloid, curli. Infect Immun 83:693–701. https://doi.org/10.1128/IAI.02370-14.
48. Kramer A, Green J, Pollard J, Jr, Tugendreich S. 2014. Causal analysis approaches in Ingenuity Pathway Analysis. Bioinformatics 30:523–530. https://doi.org/10.1093/bioinformatics/btt703.